Magnetic dynamos in white dwarfs – II. Relating magnetism and pollution

Matthias R. Schreiber,[1,2]★ Diogo Belloni [1,3] Boris T. Gänsicke [4] and Steven G. Parsons [5]

[1]*Departamento de Física, Universidad Técnica Federico Santa María, Av. España 1680, Valparaíso, Chile*
[2]*Millennium Nucleus for Planet Formation (NPF), Valparaíso, Chile*
[3]*National Institute for Space Research, Av. dos Astronautas, 1758, 12227-010 São José dos Campos, SP, Brazil*
[4]*Department of Physics, University of Warwick, Coventry CV4 7AL, UK*
[5]*Department of Physics and Astronomy, University of Sheffield, Sheffield S3 7RH, UK*

ABSTRACT

We investigate whether the recently suggested rotation and crystallization driven dynamo can explain the apparent increase of magnetism in old metal polluted white dwarfs. We find that the effective temperature distribution of polluted magnetic white dwarfs is in agreement with most/all of them having a crystallizing core, and increased rotational velocities are expected due to accretion of planetary material that is evidenced by the metal absorption lines. We conclude that a rotation and crystallization driven dynamo offers not only an explanation for the different occurrence rates of strongly magnetic white dwarfs in close binaries but also for the high incidence of weaker magnetic fields in old metal polluted white dwarfs.

Key words: magnetic fields – white dwarfs – planetary systems.

Metal absorption lines in the spectra of white dwarfs have been firmly established to result from the accretion of planetary material that survived the transformation of their host star into a white dwarf. This idea was first proposed by Jura (2003) and later confirmed to be correct due to the detection of a transiting planetesimal in the process of tidal disintegration (Vanderburg et al. 2015; Gänsicke et al. 2016). This key evidence is complemented by the detection of dusty and gaseous debris discs (e.g. Zuckerman & Becklin 1987; Gänsicke et al. 2006), a planetesimal that is possibly the core of a differentiated rocky planet (Manser et al. 2019) and an evaporating planet in close orbit around a white dwarf (Gänsicke et al. 2019).

This growing observational evidence for the accretion of planetary material on to white dwarfs is in agreement with theoretical predictions. It is well established that planets can survive the transition of their host star into a white dwarf (e.g. Villaver & Livio 2009; Ronco et al. 2020). Some of the surviving planetary systems are predicted to become unstable which can push especially lower mass planets or asteroids into highly eccentric orbits (Veras & Gänsicke 2015; Smallwood et al. 2018; Maldonado et al. 2021). Tidal forces may then destroy these objects which offers a consistent explanation for the observations of planetary material being accreted on to 25–50 per cent of all white dwarfs (Koester, Gänsicke & Farihi 2014).

As noticed by Hollands, Gänsicke & Koester (2015), very old metal polluted white dwarfs are more frequently magnetic than younger systems. All magnetic metal polluted helium (DZ) white dwarfs and all but one known magnetic metal polluted hydrogen atmosphere white dwarfs (DAZ) have effective temperatures below 7500 K (Hollands et al. 2017; Kawka et al. 2019, 2021). In addition, three apparently isolated white dwarfs exhibiting Zeeman split emission lines which might be related to the existence of a conductive planet or planet core in a close orbit, cluster around temperatures

of ∼7500 K (e.g. Li, Ferrario & Wickramasinghe 1998; Gänsicke et al. 2020; Walters et al. 2021). This suggests that the accretion of planetary material and low temperatures may be linked to the generation of magnetic fields in white dwarfs.

Inspired by the earlier work of Isern et al. (2017), we recently proposed a dynamo similar to those operating in planets and low-mass stars to explain the observed incidence of strongly magnetic white dwarfs in close binary stars (Schreiber et al. 2021). The main ingredients for this dynamo to work are that the white dwarf's core started to crystallize (which depending on the mass of the white dwarf generally occurs at white dwarf temperatures below $\simeq$ 8000 K) and increased rotational velocities due to accretion. We here test the hypothesis that the increasing fraction of magnetic white dwarfs among cold metal polluted (and therefore accreting) white dwarfs could be produced by the same dynamo mechanism. We start with a brief review of the dynamo mechanism recently suggested to work in accreting white dwarfs in close binaries.

2 THE CONVECTIVE DYNAMO APPLIED TO WHITE DWARFS

The magnetic fields of planets and rapidly rotating low-mass stars are generated by convection-driven dynamos (Christensen, Holzwarth & Reiners 2009). The main ingredients for these dynamos to work are a strong density stratification, an extended convection zone, and rotation. A similar configuration can occur in cooling white dwarfs.

As a carbon/oxygen white dwarf cools, the ions in the core begin to freeze in a lattice structure (Van Horn 1968), i.e. the white dwarf starts to crystallize. The phase diagram of the carbon–oxygen mixture is of the azeotrop form (e.g. Horowitz, Schneider & Berry 2010, Blouin et al. 2020) and consequently, the solid phase becomes richer in oxygen and sinks while the carbon excess mixes with the outer liquid envelope which is redistributed by the Rayleigh–Taylor instability

★ E-mail: matthias.schreiber@usm.cl

(e.g. Isern et al. 1997). If the white dwarf is also rapidly rotating, the conditions are appropriate for magnetic field generation through the convective dynamo.

For planets and low-mass stars, the magnetic field strength can be derived from fundamental properties of a given object using the convective energy flux scaling law (Christensen et al. 2009). Applying this scaling law to white dwarfs led to the prediction of field strengths below ~ 1 MG (Isern et al. 2017). However, the field strength generated by the dynamo likely depends on the magnetic Prandtl number (Brandenburg 2014) which is not taken into account in the scaling law (Christensen & Aubert 2006). Given that the magnetic Prandtl number for crystallizing white dwarfs is orders of magnitude larger than that of planets and low-mass stars, the field strength generated by the dynamo is likely also much larger (Bovino, Schleicher & Schober 2013). For more details, see Schreiber et al. (2021).

According to measurements of activity and rotation in fully convective stars, the dynamo seems to saturate for Rossby numbers (rotation period divided by convective turnover time) below 0.1 which might indicate that the generated field strength becomes independent of the rotation rate for rapidly spinning stars. For white dwarfs, the condition on the Rossby number translates to rotation periods of the order of seconds/minutes as the threshold for saturation. For slower rotation rates, magnetic fields might still be generated but should on average be weaker.

Based on the reasonable assumption that strong magnetic fields can be generated if a crystallizing white dwarf is rotating in the saturated regime, Schreiber et al. (2021) explained the occurrence rates and characteristics of strongly magnetic white dwarfs in close binary stars. The very same mechanism may explain the large incidence of weaker magnetic fields in cool metal polluted white dwarfs if they have temperatures consistent with crystallizing cores and if the accretion of planetary material can significantly increase their rotation. In the next section, we evaluate whether the distribution of effective temperatures of magnetic DAZ and DZ white dwarfs is consistent with them having crystallizing cores.

3 CRYSTALLIZING CORES IN MAGNETIC METAL POLLUTED WHITE DWARFS

The onset of crystallization in white dwarfs, a requirement for the dynamo mechanism proposed by Schreiber et al. (2021), depends not only on the white dwarf effective temperature but also on the white dwarf mass. However, measuring the masses of magnetic white dwarfs is extremely challenging. The standard technique for non-magnetic DA white dwarfs, which make up the bulk of the white dwarf population (e.g. McCleery et al. 2020), is to measure the effective temperature and surface gravity from fitting the Balmer lines and then to determine the white dwarf mass using a mass–radius relation. There is currently no theory for the simultaneous treatment of the Zeeman effect and Stark broadening, and therefore, this method cannot be applied to magnetic DA(Z) white dwarfs.

An alternative method to derive white dwarf masses is to iteratively fit the photometric spectral energy distribution (SED; which for a given temperature, is very sensitive to the radius) and the spectrum (where the relative strengths of absorption lines provide a handle on the temperature), and to subsequently derive the mass adopting a white dwarf mass–radius relation. However, this method requires accurate knowledge of the distance to the white dwarf under analysis. Most cool and faint DZ white dwarfs in our sample have large parallax uncertainties in the available *Gaia* data releases, and consequently, estimated masses are unreliable (Coutu et al. 2019). Additional

complications arise from the line blanketing caused by the metals in the magnetic DZ white dwarfs considered here, introducing the detailed photospheric abundances as additional free fit parameters. Finally, magnetic fields may suppress or weaken convection, which will affect the temperature structure and emerging spectrum of magnetic white dwarfs (Gentile Fusillo et al. 2018), and it is currently unclear whether the SEDs of magnetic white dwarfs are better fitted with radiative or convective models. Given the difficulties in determining the individual masses of the magnetic metal polluted white dwarfs, we here investigate whether the distribution of their effective temperatures is in agreement with their cores being in the process of crystallization.

Largely based on earlier work (Hollands et al. 2017), evidence is growing that the occurrence of magnetic fields in DZ white dwarfs increases with decreasing temperature (Kawka et al. 2021). All magnetic DZ white dwarfs have effective temperatures below 7500 K. At these low temperatures $\simeq 40$ per cent of the known DZ white dwarfs are magnetic. In contrast, not a single magnetic DZ has been found in the temperature range 7500–10 000 K. The situation is very similar for DAZ white dwarfs among which the fraction of magnetic systems increases significantly with decreasing effective temperature and all but one magnetic DAZ white dwarfs are cooler than ~7500 K. A list of magnetic DAZ and DZ white dwarfs is provided in Table 1, where we ignored some candidate magnetic systems suggested in Kawka & Vennes (2014) and Coutu et al. (2019) as well as the magnetic Balmer emission line white dwarfs discussed by Gänsicke et al. (2020).

Comparing the measured temperatures with those expected for crystallizing white dwarfs, we find good agreement with ongoing crystallization in their cores (see Fig. 1). Roughly 80 per cent of single white dwarfs can be found in the mass range of 0.5–0.75 $M_\odot$ (Tremblay et al. 2016) and the distribution peaks at $\simeq 0.6$ $M_\odot$. All magnetic DZ and all but one magnetic DAZ white dwarfs are cooler than the temperature at which a 0.75 $M_\odot$ white dwarf starts to crystallize ($\sim 8\,000$ K) and roughly half of them are below the crystallization temperature of a 0.6 $M_\odot$ white dwarf (see Fig. 1). Only the hottest ($\sim 11\,000$ K) metal polluted magnetic white dwarf, the DAZ white dwarf WD 2105−820, seems to contradict this finding as its temperature is too high to be crystallizing if its mass was that of a typical 0.5–0.75 $M_\odot$ white dwarf. However, apart from being the hottest metal polluted magnetic white dwarf, WD 2105−820 is also most likely the most massive one. Swan et al. (2019) estimated a white dwarf mass of 0.86 $M_\odot$ for which crystallization starts at much higher temperatures. The estimated mass is not high enough to reach the onset of crystallization, but assuming an uncertainty of just 0.05 $M_\odot$ would fix this apparent disagreement (which would be completely consistent with the uncertainty provided for log g). We conclude that indeed most/all metal polluted magnetic white dwarfs might have passed the onset of crystallization in their cores.

The remaining question is whether the accretion of planetary material could spin-up the white dwarfs to reach significantly increased rotational velocities.

4 SPIN-UP OF THE WHITE DWARF

The second ingredient for the proposed dynamo to work is increased rotation of the white dwarf. It is well established that metal polluted white dwarfs accrete planetary debris that result from disintegrating planetesimals, asteroids, comets, or planets. During the accretion process, the white dwarf not only accretes mass, but also angular momentum (Stephan et al. 2020). We here estimate whether the

Table 1. Currently known magnetic DZ and DAZ white dwarfs.

Name	Type	$T_{\rm eff}$ [K]	B_S [MG]	Reference
SDSS J0037−0525	DZ	5630 ± 120	7.09 ± 0.04	1
SDSS J0107+2650	DZ	6190 ± 140	3.37 ± 0.07	1
SDSS J0157+0033	DZ	6110 ± 140	3.49 ± 0.05	1
SDSS J0200+1646	DZ	5810 ± 180	10.71 ± 0.07	1
SDSS J0735+2057	DZ	6110 ± 180	6.12 ± 0.06	1
SDSS J0806+4058	DZ	6808 ± 80	0.80 ± 0.03	1
SDSS J0832+4109	DZ	6070 ± 190	2.35 ± 0.11	1
SDSS J0902+3625	DZ	6330 ± 210	1.92 ± 0.05	1
SDSS J0927+4931	DZ	6200 ± 230	2.10 ± 0.09	1
SDSS J1003-0031	DZ	5740 ± 140	4.37 ± 0.05	1
SDSS J1105+5006	DZ	7280 ± 190	4.13 ± 0.11	1
SDSS J1106+6737	DZ	6400 ± 170	3.50 ± 0.09	1
SDSS J1113+2751	DZ	6180 ± 210	3.18 ± 0.09	1
SDSS J1150+4533	DZ	5720 ± 320	2.01 ± 0.20	1
SDSS J1152+1605	DZ	6550 ± 160	2.72 ± 0.04	1
SDSS J1214−0234	DZ	5210 ± 100	2.12 ± 0.03	1
SDSS J1249+6514	DZ	7540 ± 170	2.15 ± 0.05	1
SDSS J1330+3029	DZ	6100 ± 60	0.57 ± 0.04	1
SDSS J1412+2836	DZ	4990 ± 160	1.99 ± 0.10	1
SDSS J1536+4205	DZ	5800 ± 140	9.59 ± 0.04	1
SDSS J1546+3009	DZ	6600 ± 120	0.81 ± 0.07	1
SDSS J1651+4249	DZ	5710 ± 200	3.12 ± 0.28	1
SDSS J2254+3031	DZ	5900 ± 90	2.53 ± 0.03	1
SDSS J2325+0448	DZ	6020 ± 100	6.56 ± 0.09	1
SDSS J2330+2805	DZ	6670 ± 210	3.40 ± 0.04	1
WD 1515+8230	DZ	4360 ± 80	3.1 ± 0.2	2
WD 0816−310	DZ	6436	0.092 ± 0.001	3,4,5
WD 1009−184	DZ	6036	$\gtrsim 0.3$	3,6
WD 1532+129	DZ	5430	$\gtrsim 0.3$	3,4
WD 2138−332	DZ	7399	$\gtrsim 0.4$	3,4
WD 0214−071	DAZ	5460 ± 40	0.163 ± 0.004	7
WD 0315−293	DAZ	5200 ± 200	0.519 ± 0.04	7,8,9
WD 0322−019	DAZ	5310 ± 100	0.120	7,10,11
WD 1653+385	DAZ	5900	0.07	7,12
WD 2225+176	DAZ	6250 ± 70	0.334 ± 0.003	7,13
WD 2105−820	DAZ	10890 ± 380	$\simeq 0.043$	7,14,15,16

Note. References: (1) Hollands et al. (2017), (2) Tremblay et al. (2020), (3) Bagnulo & Landstreet (2019), (4) Giammichele, Bergeron & Dufour (2012), (5) Kawka et al. (2021), (6) Subasavage et al. (2017), (7) Kawka et al. (2019), (8) Kawka & Vennes (2012), (9) Kawka & Vennes (2011), (10) Farihi et al. (2011), (11) Farihi et al. (2018), (12) Zuckerman et al. (2011), (13) Kawka & Vennes (2014), (14) Koester et al. (1998), (15) Landstreet et al. (2012), (16) Swan et al. (2019).

Figure 1. The onset and 80 per cent completed crystallization temperatures for thin (blue) and thick (black) hydrogen atmospheres taken from Bédard et al. (2020). For thin atmospheres (DZ), crystallization starts at slightly higher temperatures than for thick atmospheres (DAZ). Crystallization starts at effective temperatures well above 10 000 K for massive white dwarfs but for typical white dwarf masses in the range 5000–9000 K. The currently known DZ (blue histogram) and DAZ (grey histogram) magnetic white dwarfs lie exactly in the temperature range of crystallizing cores for typical white dwarf masses. The only exception is WD 2105–820 which is hotter and (most likely and fittingly) more massive (Swan et al. 2019).

a rare event. For planetary systems consisting of five or six planets, star–planet collisions are expected in ∼10 per cent of the cases.

The accretion of planetary material does not only lead to metal absorption lines in the spectra of white dwarfs, accretion of mass is accompanied by the accretion of angular momentum. The material from destroyed planetesimals, asteroids, comets, and planets accumulates in a Keplerian disc around the white dwarf and is then slowly accreted on to the white dwarf. King, Regev & Wynn (1991) derived the angular momentum balance equation for accreting white dwarfs in cataclysmic variables (CVs) and found

$$I \frac{d\omega}{dt} = \alpha \left(-\dot{M}_2 \right) \left(G M_{\rm WD} R_{\rm WD} \right)^{1/2} + (1 + \epsilon) \left(\dot{M}_2 \eta R_{\rm WD}^2 \omega \right), \tag{1}$$

where ω is the white dwarf spin, I its moment of inertia, G the gravitational constant, $\dot{M}_2$ the mass transfer rate averaged over nova cycles, and $M_{\rm WD}$ and $R_{\rm WD}$ are the white dwarf mass and radius. The first term on the right-hand side of the equation corresponds to the spin-up due to accretion and the parameter $0 \leq \alpha \leq 1$ (added by Schreiber et al. 2021) represents the spin-up efficiency. The second term represents the spin-down due to material leaving the white dwarf which can be ignored in this work as nova eruptions are generally not expected ($\epsilon = -1.0$) given the small amount of accreted hydrogen (the accretion of an entire Jupiter mass planet could be a rare exception). We solved the non-homogeneous differential equation (1) as in Schreiber et al. (2021) for total accreted mass (over a time span of several Gyr) of $10^{-6} - 10^{-3}$ M$_\odot$ which roughly covers the mass range from Earth to Jupiter.

We find that the accretion of planetary material in polluted white dwarfs can easily lead to significantly shorter spin periods. Figure 2 shows the spin-up of a 0.6 M$_\odot$ white dwarf for different total accretion rates as a function of the spin-up efficiency. For accreted masses exceeding 10^{-5} M$_\odot$, we find rotation periods ranging from several minutes, as recently observed (Reding et al. 2020), to a few hours, much shorter than the assumed initial rotation rate of 1–3 d (Hermes

accreted angular momentum might sufficiently spin-up the white dwarf to cause the generation of detectable magnetic fields.

From a large sample of cold and old metal polluted white dwarfs, Hollands et al. (2017) derived a trend of decreasing accretion rates with an e-folding time of $\simeq 1$ Gyr. This observed long term trend, however, does not cover short episodes of much larger accretion rates that occur when rocky or even gas giant planets come too close to the white dwarfs. Observational evidence for such events has been provided recently (Gänsicke et al. 2019; Manser et al. 2019). In addition, the recently observed giant planet around WD 1856+534 shows that even Jupiter mass planets may end up in close orbits around white dwarfs either due to common envelope evolution (Lagos et al. 2021), triple dynamics (Muñoz & Petrovich 2020), or gravitational interactions (Maldonado et al. 2020). Indeed, using configurations of planetary systems derived from observed systems, Maldonado et al. (2020) showed that eccentricity pumping leading to the tidal disruption and/or evaporation of planets is by no means
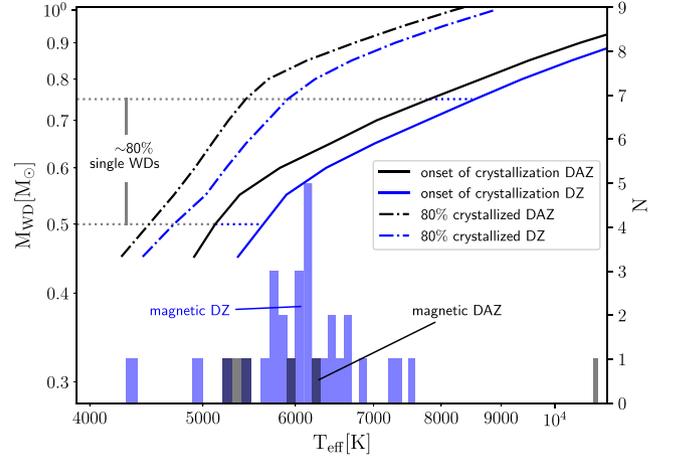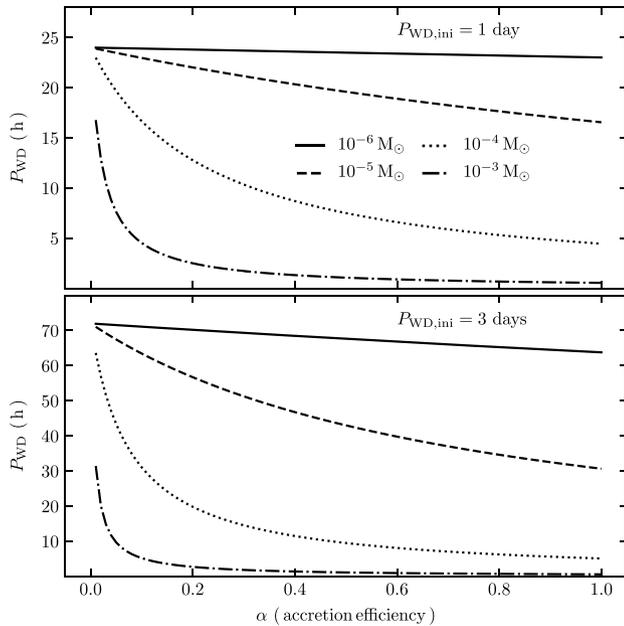
Figure 2. Final white dwarf spin period (P_{WD}) against the spin-up efficiency parameter (α), for four different accreted masses, in $M_\odot$, namely 10^{-6}, 10^{-5}, 10^{-4}, and 10^{-3} and two initial spin periods. With the exception of accreted masses $\lesssim 10^{-5}$, the white dwarf spin periods become significantly shorter (minutes to a few hours) for a large range of efficiencies.

Figure 3. Predicted temperature distributions of crystallizing DAZ and DZ white dwarfs assuming solar metallicity and a constant occurrence rate of planetary systems around progenitor stars less massive then 3.0 $M_\odot$. The predicted distribution of temperatures of DZ white dwarfs is much broader and peaks at higher temperatures than the observed DZ sample.

et al. 2017). At the same time, the spin periods reached remain longer than the spin period estimated by Isern et al. (2017) for saturation of the dynamo which could be reached due to the accretion of significantly more mass in CVs. One would therefore expect the generated magnetic fields in DZ and DAZ white dwarfs to be weaker than the up to several 100 MG fields of strongly magnetic white dwarfs in CVs which is clearly the case (see Table 1).

We conclude that both conditions for the generation of magnetic fields due to a crystallization and rotation driven dynamo are most likely fulfilled in DZ and DAZ white dwarfs. To the best of our knowledge, no other scenario suggested for the generation of magnetic fields in white dwarfs offers an explanation for the increased incidence of magnetism in old metal polluted white dwarfs.

However, in the absence of a scaling law that takes into account the dependence on the magnetic Prandtl number, let alone detailed simulations of the dynamo in white dwarfs, we admit that the presented arguments are reasonable but phenomenological. More detailed theoretical investigations as well as a representative sample of observed magnetic DZ and DAZ white dwarfs are clearly required to further test the outlined scenario.

5 PREDICTIONS TO BE TESTED

At first glance, one might think that calculating the temperature distribution of crystallizing white dwarfs by combining stellar evolution codes and white dwarf cooling tracks could be an easy way to confront the observed temperature distribution with model predictions. However, such a comparison would currently represent a rather futile exercise as the distributions of the effective temperatures of the currently available sample of DAZ and DZ white dwarfs is not only very likely biased towards hot white dwarfs but also incomplete. In addition, making reliable model predictions for the temperature distribution of crystallizing metal polluted white dwarfs is currently
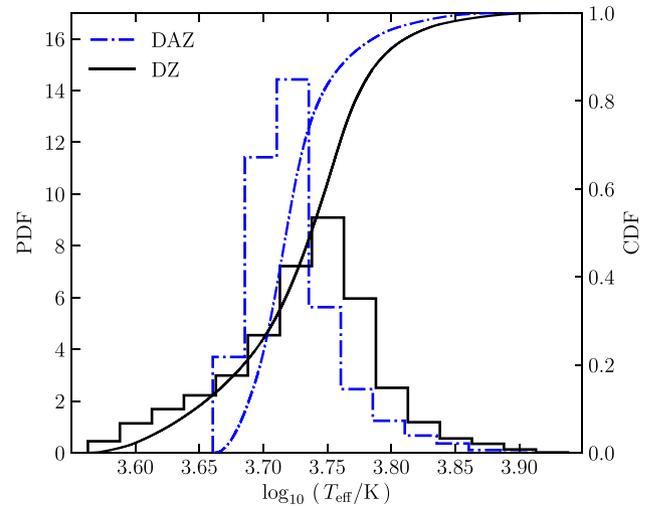
hardly possible as the occurrence rate of planetary systems around the progenitor stars and its exact dependence on the stellar mass, planet separation, planet mass, and stellar metallicity are, despite recent progress (e.g. Fischer & Valenti 2005; Mulders, Pascucci & Apai 2015), not well known. Therefore, instead of performing such a comparison, we here investigate whether the suggested dynamo scenario leads to predictions that can be observationally tested in the near future.

To that end, we calculated the temperature distribution of crystallizing DZ and DAZ white dwarfs for solar metallicity and assuming a constant probability for the existence of planetary systems up to masses of the white dwarf progenitor of 3.0 $M_\odot$. As the planet occurrence rate seems to drop for larger stellar masses (e.g. Mulders et al. 2015), we assumed that planets do not form around more massive stars. We furthermore assumed a constant star formation rate, an age of the Galactic disc of 10 Gyr, and an initial mass function $\propto M^{-2.3}$. We used the the single star evolution code written by Hurley, Pols & Tout (2000) and the white dwarf cooling models of Bédard et al. (2020).

The resulting temperature distributions are shown in Fig. 3. As the onset of crystallization for DZ white dwarfs occurs at higher temperatures, their distribution peaks at a slightly higher temperature. Given that, in addition, the late cooling of DZ white dwarfs is faster, their predicted distribution also extends more towards cooler white dwarfs. While the detailed shape of both distributions depends on the assumed occurrence rate of planets as a function of stellar mass and metallicity, the predicted differences should be present as long as both samples suffer from the same observational biases and their progenitor stars have the same planet occurrence rates.

The small number of magnetic DAZ and DZ white dwarfs currently known does not allow us to asses whether the underlying temperature distributions are different. However, the ongoing SDSS-V survey will provide spectra of $\sim 200\,000$ white dwarfs, many of which will be metal polluted and a significant fraction of the latter will be magnetic. Thus, the required large sample of magnetic DZ and DAZ white dwarfs is likely to be established within the next few years.

A second and obvious prediction of our model is that the rotation periods of magnetic DZ and DAZ white dwarfs should be on average shorter than those of non-magnetic white dwarfs with crystallizing cores. Fortunately, the rotation periods of magnetic white dwarfs can be measured through either photometric variability (Brinkworth et al. 2013) or circular spectropolarimetry of spectral lines (Bagnulo & Landstreet 2019) and thus the prediction can be tested. Interestingly, the three cold magnetic white dwarfs showing Balmer emission and potentially hosting a conductive planet or planetary core (Gänsicke et al. 2020) clearly show reduced spin periods, which fits with the scenario outlined here.

Our scenario also predicts that a certain fraction of crystallizing white dwarfs currently not showing metal absorption lines should have increased rotation rates and be magnetic because accretion that spun up the white dwarf has occurred in the past. The cool magnetic white dwarfs found in the 20 pc sample (Bagnulo & Landstreet 2020) could be such systems.

Finally, another mechanism must be responsible for the magnetic fields observed in some hot white dwarfs and this alternative process must prevent the accretion of planetary debris (given the absence of hot magnetic metal polluted white dwarfs). Double white dwarf mergers could be such a mechanism, as planetary material is certainly unlikely to survive two phases of mass transfer.

6 CONCLUSION

Schreiber et al. (2021) recently suggested a crystallization and rotation driven dynamo for the origin of strong magnetic fields of white dwarfs in close binary stars. We here investigated whether the same mechanism might be responsible for the surprising increase of magnetism in metal polluted white dwarfs when they have cooled to temperatures ≲ 7500 K. We found that the temperature distribution of metal polluted magnetic DAZ and DZ white dwarfs is consistent with them having crystallizing cores and that the accretion of planetary material can spin-up the white dwarf's rotation to periods ranging from minutes to hours depending on the total amount of accreted material. Thus, the suggested dynamo represents a promising model for explaining the magnetic fields of old DA/DAZ white dwarfs.

DATA AVAILABILITY

The simulated data will be provided upon request.

REFERENCES

Bagnulo S., Landstreet J. D., 2019, A&A, 630, A65
Bagnulo S., Landstreet J. D., 2020, A&A, 643, A134
Bédard A., Bergeron P., Brassard P., Fontaine G., 2020, ApJ, 901, 93
Blouin S., Daligault J., Saumon D., Bédard A., Brassard P. (2020) A&A L11, , 0004-6361
Bovino S., Schleicher D. R. G., Schober J., 2013, New J. Phys., 15, 013055

Brandenburg A., 2014, ApJ, 791, 12
Brinkworth C. S., Burleigh M. R., Lawrie K., Marsh T. R., Knigge C., 2013, ApJ, 773, 47
Christensen U. R., Aubert J., 2006, Geophys. J. Int., 166, 97
Christensen U. R., Holzwarth V., Reiners A., 2009, Nature, 457, 167
Coutu S., Dufour P., Bergeron P., Blouin S., Loranger E., Allard N. F., Dunlap B. H., 2019, ApJ, 885, 74
Farihi J. et al., 2018, MNRAS, 474, 947
Farihi J., Dufour P., Napiwotzki R., Koester D., 2011, MNRAS, 413, 2559
Fischer D. A., Valenti J., 2005, ApJ, 622, 1102
Gänsicke B. T. et al., 2016, ApJ, 818, L7
Gänsicke B. T., Marsh T. R., Southworth J., Rebassa-Mansergas A., 2006, Science, 314, 1908
Gänsicke B. T., Rodríguez-Gil P., Gentile Fusillo N. P., Inight K., Schreiber M. R., Pala A. F., Tremblay P.-E., 2020, MNRAS, 499, 2564
Gänsicke B. T., Schreiber M. R., Toloza O., Fusillo N. P. G., Koester D., Manser C. J., 2019, Nature, 576, 61
Gentile Fusillo N. P., Tremblay P. E., Jordan S., Gänsicke B. T., Kalirai J. S., Cummings J., 2018, MNRAS, 473, 3693
Giammichele N., Bergeron P., Dufour P., 2012, ApJS, 199, 29
Hermes J. J. et al., 2017, ApJS, 232, 23
Hollands M. A., Gänsicke B. T., Koester D., 2015, MNRAS, 450, 681
Hollands M. A., Koester D., Alekseev V., Herbert E. L., Gänsicke B. T., 2017, MNRAS, 467, 4970
Horowitz C. J., Schneider A. S., Berry D. K., 2010, Phys. Rev. Lett., 104, 231101
Hurley J. R., Pols O. R., Tout C. A., 2000, MNRAS, 315, 543
Isern J., García-Berro E., Külebi B., Lorén-Aguilar P., 2017, ApJ, 836, L28
Isern J., Mochkovitch R., García-Berro E., Hernanz M., 1997, ApJ, 485, 308
Jura M., 2003, ApJ, 584, L91
Kawka A., Vennes S., 2011, A&A, 532, A7
Kawka A., Vennes S., 2012, A&A, 538, A13
Kawka A., Vennes S., 2014, MNRAS, 439, L90
Kawka A., Vennes S., Allard N. F., Leininger T., Gadéa F. X., 2021, MNRAS, 500, 2732
Kawka A., Vennes S., Ferrario L., Paunzen E., 2019, MNRAS, 482, 5201
King A. R., Regev O., Wynn G. A., 1991, MNRAS, 251, 30P
Koester D., Dreizler S., Weidemann V., Allard N. F., 1998, A&A, 338, 612
Koester D., Gänsicke B. T., Farihi J., 2014, A&A, 566, A34
Lagos F., Schreiber M. R., Zorotovic M., Gänsicke B. T., Ronco M. P., Hamers A. S., 2021, MNRAS, 501, 676
Landstreet J. D., Bagnulo S., Valyavin G. G., Fossati L., Jordan S., Monin D., Wade G. A., 2012, A&A, 545, A30
Li J., Ferrario L., Wickramasinghe D., 1998, ApJ, 503, L151
Maldonado R. F., Villaver E., Mustill A. J., Chávez M., Bertone E., 2021, MNRAS, 501, L48
Manser C. J. et al., 2019, Science, 364, 66
McCleery J. et al., 2020, MNRAS, 499, 1890
Mulders G. D., Pascucci I., Apai D., 2015, ApJ, 814, 130
Muñoz D. J., Petrovich C., 2020, ApJ, 904, L3
Reding J. S., Hermes J. J., Vanderbosch Z., Dennihy E., Kaiser B. C., Mace C. B., Dunlap B. H., Clemens J. C., 2020, ApJ, 894, 19
Ronco M. P., Schreiber M. R., Giuppone C. A., Veras D., Cuadra J., Guilera O. M., 2020, ApJ, 898, L23
Schreiber M. R., Belloni D., Gänsicke B. T., Parsons S. G., Zorotovic M., 2021, Nat. Astron.
Smallwood J. L., Martin R. G., Livio M., Lubow S. H., 2018, MNRAS, 480, 57
Stephan A. P., Naoz S., Gaudi B. S., Salas J. M., 2020, ApJ, 889, 45
Subasavage J. P. et al., 2017, AJ, 154, 32
Swan A., Farihi J., Koester D., Hollands M., Parsons S., Cauley P. W., Redfield S., Gänsicke B. T., 2019, MNRAS, 490, 202
Tremblay P. E. et al., 2020, MNRAS, 497, 130

Tremblay P. E., Cummings J., Kalirai J. S., Gänsicke B. T., Gentile-Fusillo N., Raddi R., 2016, MNRAS, 461, 2100

van Horn H. M., 1968, ApJ, 151, 227

Vanderburg A. et al., 2015, Nature, 526, 546

Veras D., Gänsicke B. T., 2015, MNRAS, 447, 1049

Villaver E., Livio M., 2009, ApJ, 705, L81

Walters N. et al., 2021, MNRAS, 503, 3743

Zuckerman B., Becklin E. E., 1987, Nature, 330, 138

Zuckerman B., Koester D., Dufour P., Melis C., Klein B., Jura M., 2011, ApJ, 739, 101

This paper has been typeset from a TEX/LATEX file prepared by the author.